Liquid Crystals
Publication details, including instructions for authors and subscription information:
http://www.informaworld.com/smpp/title~content=t713926090

Transition moment orientation and rotational bias of three carbonyl groups in large polarization FLCs observed by polarized FTIR

J. Matsushima; Y. Takanishi; K. Ishikawa; H. Takezoe; A. Fukuda; C. S. Park; W. G. Jang; K. H. Kim; J. E. MacLennan; M. A. Glaser; N. A. Clark; K. Takahashi

Online publication date: 11 November 2010

To cite this Article Matsushima, J. , Takanishi, Y. , Ishikawa, K. , Takezoe, H. , Fukuda, A. , Park, C. S. , Jang, W. G. , Kim, K. H. , MacLennan, J. E. , Glaser, M. A. , Clark, N. A. and Takahashi, K.(2002) 'Transition moment orientation and rotational bias of three carbonyl groups in large polarization FLCs observed by polarized FTIR', Liquid Crystals, 29: 1, 27 — 37

To link to this Article: DOI: 10.1080/02678290110039525

URL: http://dx.doi.org/10.1080/02678290110039525

LIQUID CRYSTALS, 2002, VOL. 29, NO. 1, 27–37

Transition moment orientation and rotational bias of three carbonyl groups in large polarization FLCs observed by polarized FTIR

J. MATSUSHIMA, Y. TAKANISHI, K. ISHIKAWA, H. TAKEZOE, A. FUKUDA

Department of Organic and Polymeric Materials, Tokyo Institute of Technology, O-okayama, Meguro-ku, Tokyo 152-8552, Japan

C. S. PARK, W. G. JANG*, K. H. KIM, J. E. MACLENNAN, M. A. GLASER, N. A. CLARK

Physics Department, University of Colorado, Campus Box 390, Boulder, CO 80309-0390, USA

and K. TAKAHASHI

NTT Lifestyle and Environmental Technology Laboratory, Morinosato Wakamiya, Atsugishi 243-0198, Japan

(*Received 6 November 2000; accepted 18 December 2000*)

Polarized FTIR measurements have been made on four ferroelectric liquid crystal compounds which have a large spontaneous polarization; two of them have a hydroxyl group that can form a hydrogen bond. Particular attention was given to three C=O stretching peaks: keto, ester, and lactic acid. We found that the polar absorbance pattern and peak positions of the keto C=O group stretching vibration are clearly different in compounds with and without the hydroxyl group. We have succeeded in interpreting these measurements by calculating IR transition moment directions for the vibrational modes of several model compounds using quantum chemical methods, including HF/6-311G SCF and B3LYP/6-31G(d) and B3LYP/6-31G(d,f) DFT calculations. Rotational bias was clearly observed even in the ester C=O group in the molecular core in the SmC* phase of the compound with a hydrogen bond.

1. Introduction

Ferroelectric liquid crystals (FLCs) are characterized by their fast electro-optic response, with a response time proportional to the viscosity and inversely proportional to the spontaneous polarization, $\mathbf{P}_s$. One of the goals of FLC materials development has been to obtain compounds with large $\mathbf{P}_s$ values. Synthetic chemists have succeeded in obtaining compounds with $\mathbf{P}_s$ more than two orders of magnitude larger than that of the first FLC material, DOBAMBC. Among them, one of the compounds derived from lactic acid by Kobayashi *et al.* [1] has the largest known $\mathbf{P}_s$ of about 1 $\mu C/cm^2$. This amounts to 70–80% of $\mathbf{P}_0$, the $\mathbf{P}_s$ value calculated for perfect orientational order of molecular dipoles. This is surprising, because it suggests that the orientational distribution of the molecules about the mean molecular long axis is extremely biased.

Such biased orientation was first proved experimentally by Kim *et al.* [2] using polarized FTIR. The orientational distribution function of particular carbonyl groups on several other FLC compounds behaves similarly [3–8]. In this paper, we apply this technique to FLC compounds with an alkanoyl group. The compounds contain three C=O groups, some of which are expected to contribute to the transverse dipole. We find that the dependence of the absorbance on the incident polarization direction is different for the three C=O groups. In particular, the keto C=O absorption profile shows marked differences for compounds with and without a hydrogen bond. We discuss the molecular

*Author for correspondence; e-mail: gun@bly.colorado.edu

Liquid Crystals ISSN 0267-8292 print/ISSN 1366-5855 online © 2002 Taylor & Francis Ltd
http://www.tandf.co.uk/journals
DOI: 10.1080/02678290110039525

configuration and the rotational bias based on the polarization dependence of IR absorption intensities of C=O stretching vibrational bands.

2. Experimental

The FLC compounds studied are shown in figure 1 with their phase sequences on cooling. All the compounds exhibit monotropic SmC* phases. The structures are denoted as $OH_{m,n}$ or $noOH_{m,n}$ depending on the presence or absence of a hydroxyl group (OH) on the phenyl ring and the length m (=6 or 8) or n (=2 or 6) of the alkoxy and alkyl chains, respectively. These compounds possess three C=O groups, i.e. keto, lactic acid and ester, the first two of which are linked to chiral carbons and contribute to a large $\mathbf{P}_s$. The absolute values of $\mathbf{P}_s$ are 665, 440, 512 and 350 nC cm^{-2} in the descending order in which the compounds appear in figure 1.

FTIR measurements were performed independently at the Tokyo Institute of Technology (TIT) and at the University of Colorado (CU). In the TIT experiments, homogeneously aligned samples were prepared between two SrF_2 plates (2 mm thick) coated with indium tin oxide (ITO), which are transparent in the visible and infrared region ($\lambda = 0.13$–$11\,\mu m$). These plates were coated with polyimide (SP-550, Toray), and one of the substrates was rubbed unidirectionally. The cell thickness was held between 4.7 and 6.2 μm by using PET films as spacers. The cell was placed in an oven whose temperature was controlled within ±0.02°C. The alignment quality was checked by polarizing optical microscopy (POM) before and after the measurements. Polarized infrared absorption spectra were measured as a function of polarizer rotation angle using a JEOL JIR-WINSPEC 50 system equipped with an MCT detector. A wire-grid polarizer (Cambridge Physical Science, IGP 227) was rotated about the axis of the IR beam.

At CU, homogeneously aligned samples were prepared between CaF_2 plates (also 2 mm thick) coated with 100 Å thick ITO, which are transparent in the range $\lambda = 0.13$–$12\,\mu m$. These plates were coated with 200 Å thick nylon (elvamide), and one of the substrates was rubbed unidirectionally. The smectic phases were aligned into the bookshelf geometry, with the layers normal to the rubbing, and normal or nearly normal to the plates, the latter induced by field application or by slow cooling from the isotropic phase. The cell thickness was held between 2 and 5 μm using silica balls as spacers. The cells were also placed in an oven with ±0.02°C temperature control and the alignment quality was checked optically before and after the measurements. Measurements were made using a Bruker IFS66 spectrometer with MCT and Si detectors.

The TIT and CU data sets were quantitatively consistent and have been combined to produce the results presented here.

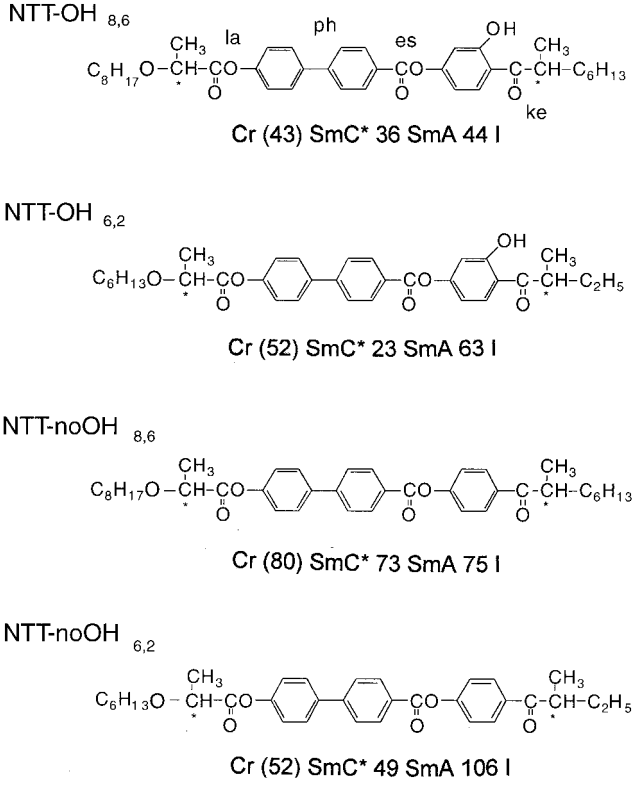

Figure 1. Structural formulae of the liquid crystal materials used and their phase sequences on cooling.

3. Experimental results

3.1. *FTIR measurements in SmA*

Figure 2 sketches the experimental geometry and shows FTIR absorption spectra for wave numbers in the neighbourhood of 1600 cm^{-1} for polarized light parallel and perpendicular to the smectic layer normal, in the SmA phase for the compounds $NTT\text{-}OH_{8,6}$ and $NTT\text{-}noOH_{8,6}$. The only clear difference between the two compounds appears in the peaks at 1635 cm^{-1} in $NTT\text{-}OH_{8,6}$ and at 1683 cm^{-1} in $NTT\text{-}noOH_{8,6}$, both assigned to the keto C=O stetching and mutually shifted because of the presence or absence of the OH group. This suggests that hydrogen bonding plays an important role for the keto C−O stretching band. The other important peaks and their assignments are given in table 1. As shown in figure 2 and table 1, the three C=O stretching peaks and a phenyl C−C stretching peak are fairly well separated, so that the polarization dependence of the IR absorption at these peaks can be accurately measured.

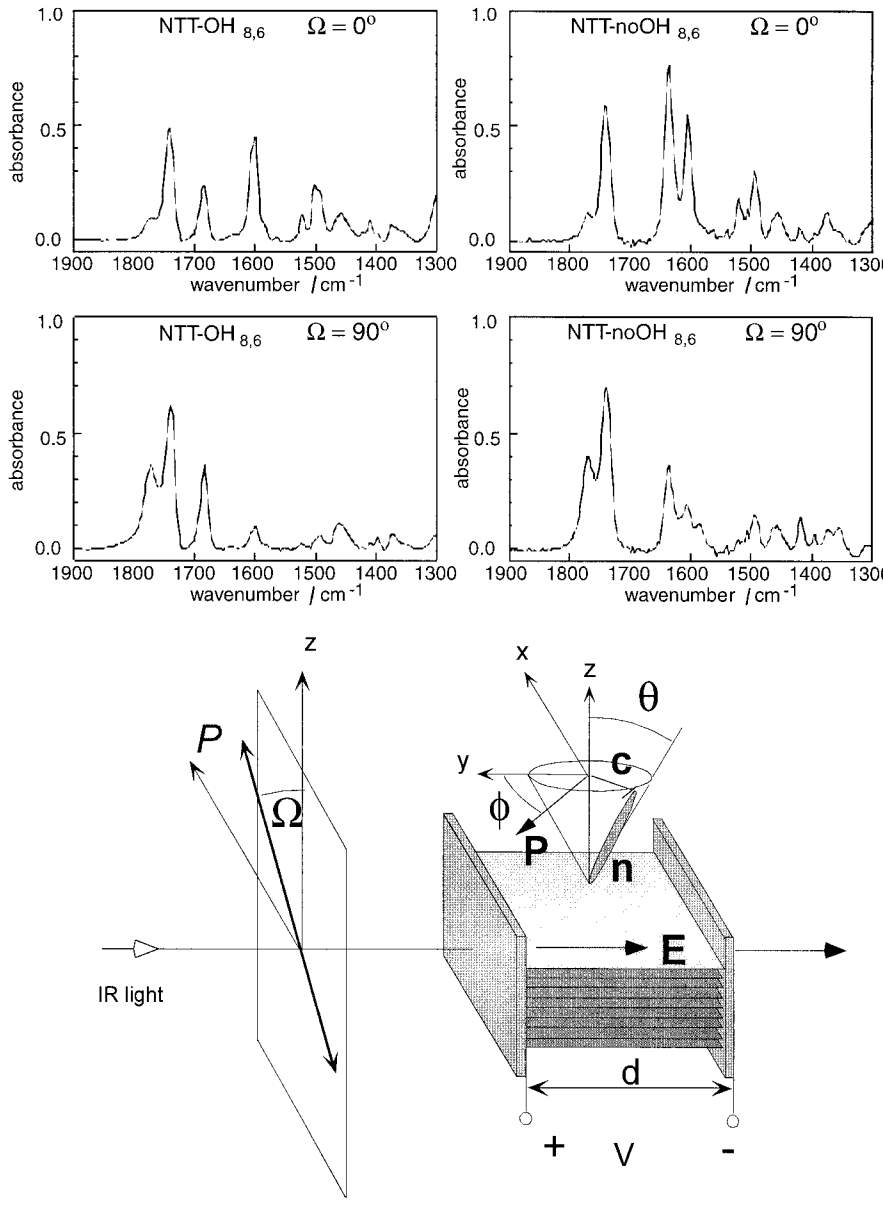

Figure 2. IR absorption spectra of NTT-$OH_{8,6}$ and NTT-$noOH_{8,6}$ for polarizations parallel and perpendicular to the layer normal in the SmA-phase. The experimental geometry is also shown.

Table 1. Main absorption peaks analysed in the present work.

Assignment	Observed wave numbers/ cm^{-1}
Phenyl ring C−C stretching	1604
Keto C=O group stretching	1635 ($OH_{m,n}$), 1683 ($noOH_{m,n}$)
Ester C=O group stretching	1741
Lactic acid C=O group stretching	1770

Figure 3 shows the absorbance vs. polarizer rotation angle Ω in the SmA phase of the four compounds without an electric field. The orientation $\Omega = 0°$ corresponds to incident polarization parallel to the layer normal direction. Overlapped peaks were deconvoluted into individual peaks and their absorbances measured. The average C−C stretching direction of the phenyl ring (ph) is parallel to the molecular long axis (the director) [2] and the layer normal in the SmA phase. The observed absorbance profiles for each mode can be qualitatively understood in terms of β, the angle between its absorption dipole and the molecular long axis. If the C=O groups rotate freely about the molecular long axis, the angular dependence of the C=O peaks should be symmetric with respect to the director [2, 3, 8]. This is in fact the case in the SmA phase. Under the condition of free rotation, A_{max} is at $\Omega = 90°(0°)$ for $\beta > (<)\beta_{magic}$, where β_{magic} is the 'magic angle', $\beta = 54.7°$, for which a

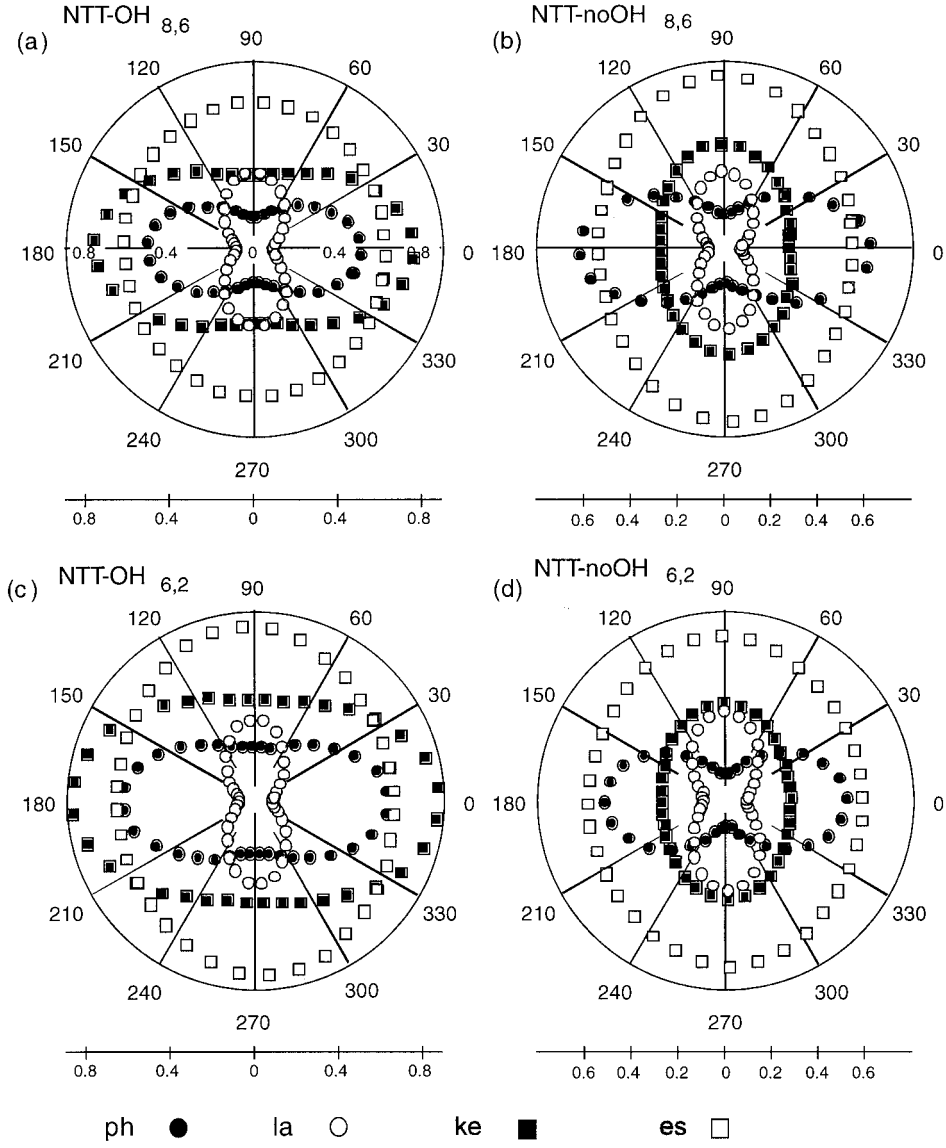

Figure 3. Absorbance vs. polarizer rotation angle for four representative stretching peaks in the SmA phase of (*a*) NTT-$OH_{8,6}$, (*b*) NTT-no$OH_{8,6}$, (*c*) NTT-$OH_{6,2}$ and (*d*) NTT-no$OH_{6,2}$.

uniaxial distribution around the long axis appears isotropic. Hence carbonyl stretching vibrations, with β in the range $\beta \sim 60°$, have A_{max} at $\Omega = 90°$.

The following features should be noted in figure 3. (1) The absorbance of the lactic acid C=O group ($\beta \sim 80°$) and the ester C=O group stretching peaks is a maximum for $\Omega = 90°$, whereas it is a maximum at $\Omega = 0°$ for the phenyl ring C=C stretching peak, although the anisotropy of the ester C=O group (particularly of $OH_{m,n}$) is very small. This feature is similar to that seen in other ferroelectric and antiferroelectric (SmC^*_A) liquid crystals in the SmA and SmC^*_A phases without an electric field [2, 4]. (2) In no$OH_{m,n}$, the angular dependence maximum of the keto C=O group stretching peak is at $\Omega = 90°$, figures 3(*b*) and 3(*d*), while it is at $\Omega = 0°$ in $OH_{m,n}$, figures 3(*a*) and 3(*c*).

3.2. *FTIR measurements in SmC**

We now discuss the changes in the IR polar absorbance pattern induced by applying an electric field in the SmC* phase. Figures 4(*a*) and 4(*b*) show the absorbance vs. polarizer rotation angle Ω in the SmC* phase (35.8°C) of NTT-$OH_{8,6}$ in a d.c. electric field of $+2.8$ and -2.8 V μm^{-1}, respectively. The corresponding pattern in the SmA phase is shown in figure 3(*a*). In an electric

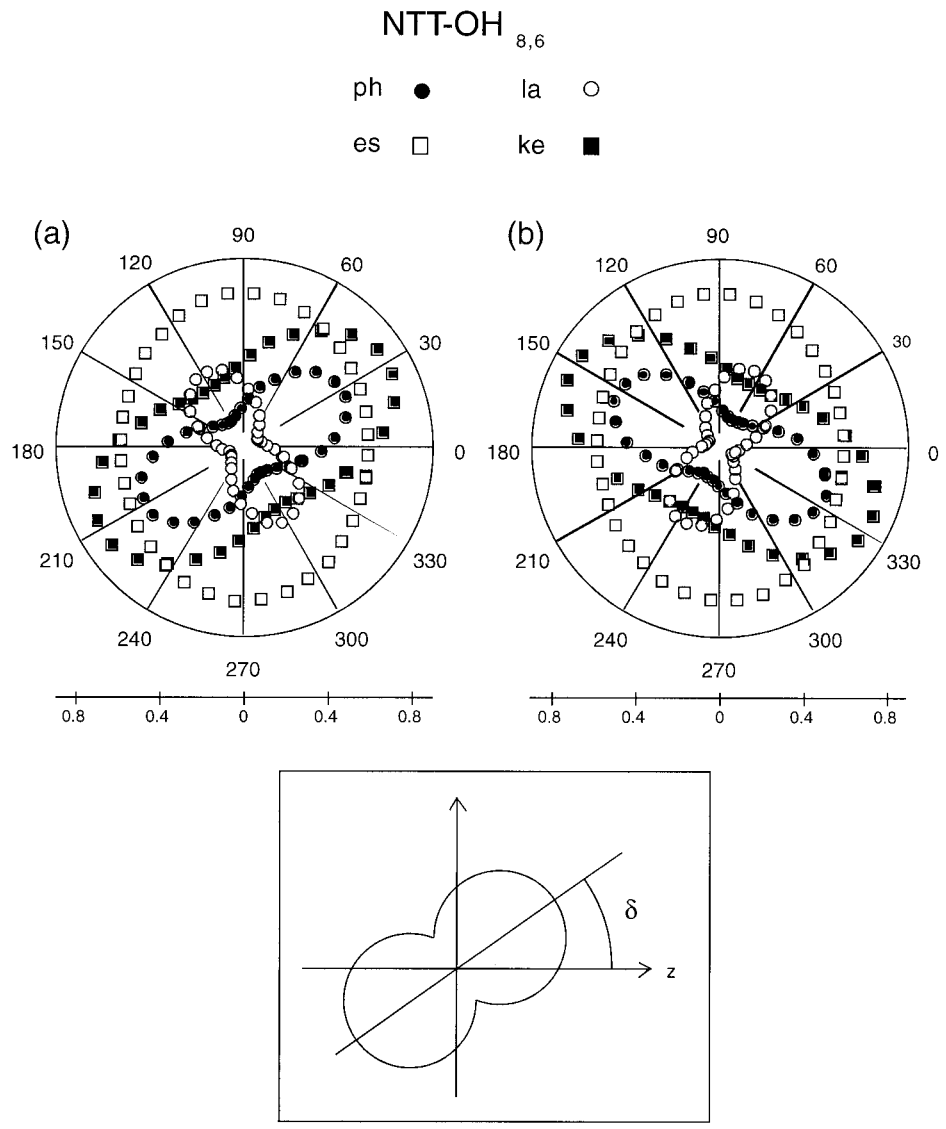

Figure 4. Absorbance vs. polarizer rotation angle for four representative stretching peaks in the SmC* phase of NTT-$OH_{8,6}$ in electric fields of (*a*) + 2.8 and (*b*) − 2.8 V μm^{-1}. Phenyl ring (closed circle), keto (closed square), ester (open square), and lactic acid (open circle) C=O stretching.

field, the average (ph) C−C stretching direction rotates from the layer normal by an angle δ defined in figure 4 comparable to the mean tilt of the molecular long axis $\theta \sim 30°$.

The angular dependence of the keto C=O group is almost symmetric with respect to the director (given by the symmetry axis of the phenyl absorption profile). In contrast, the maximum absorption of the lactic acid C=O stretching is shifted slightly from the direction perpendicular to that of the (ph) C−C symmetry axis. The maximum absorption of the ester C=O stretching scarcely rotates upon field application, though the angular anisotropy increases slightly. Such asymmetric polarization angle dependence with respect to the (ph) C−C stretching clearly indicates the biased rotation of the C=O groups around the molecular long axis [2, 4, 8].

3.3. *Smectic layer thickness*

X-ray diffraction was used to probe the temperature dependence of the layer thickness d(Å) in the four compounds, with the results shown in figure 5. The spacings of compounds NTT-$OH_{8,6}$ and NTT-no$OH_{8,6}$ clearly exhibit a jump at the SmA–SmC* phase transition temperature, indicating a first order SmA–SmC* transition. The compound NTT-$OH_{6,2}$ has a wide SmA temperature range and shows a second order transition to the SmC* phase. The SmA–SmC* transition was not actually observed in NTT-$OH_{6,2}$.

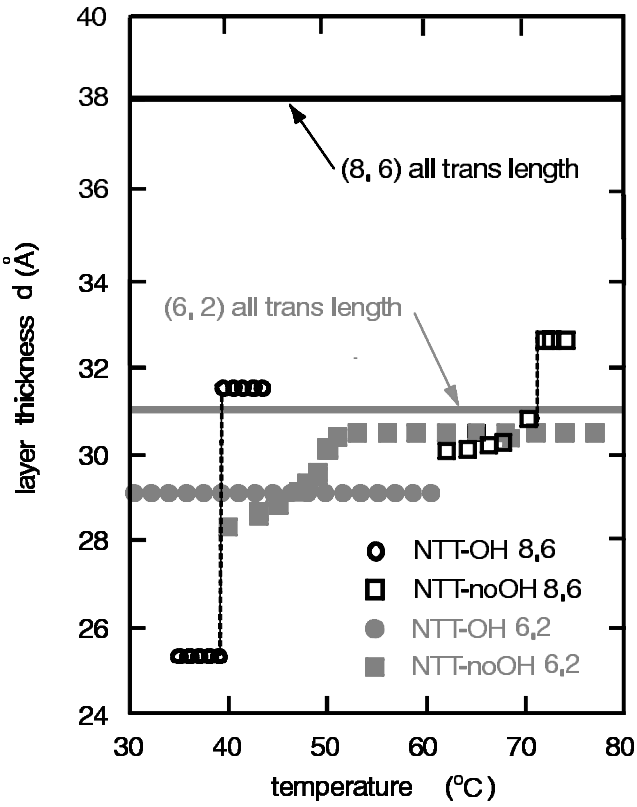

Figure 5. Smectic layer thicknesses d (Å) vs. temperature (°C). NTT-$OH_{8,6}$ (open circle), NTT-no$OH_{8,6}$ (closed circle), NTT-$OH_{6,2}$ (open square) and NTT-no$OH_{6,2}$ (closed square) compounds. In NTT-$OH_{8,6}$, NTT-no$OH_{8,6}$, and NTT-no$OH_{6,2}$ there is a layer thickness change at the SmA–SmC* phase transition, but in NTT-$OH_{6,2}$ there is no layer thickness change at this phase transition.

Another remarkable feature is that the layer thicknesses of NTT-no$OH_{8,6}$ and NTT-no$OH_{6,2}$ are much larger than those of NTT-$OH_{8,6}$ and NTT-$OH_{6,2}$, respectively. Since the molecular structures of $OH_{m,n}$ and no$OH_{m,n}$ differ only by the presence or absence of OH, this suggests that they have different local configurations. Table 2 shows the experimentally measured layer thickness in the SmA phase and the molecular length calculated assuming an all-*trans*-configuration. It is clear that the layer thicknesses in the SmA phase are nearly the same as the lengths of the molecules with all-*trans*-configurations for NTT-$OH_{6,2}$ and NTT-no$OH_{6,2}$. However, the measured layer thicknesses of NTT-$OH_{8,6}$ and NTT-no$OH_{8,6}$ are considerably shorter than the lengths calculated with our all-*trans*-configuration, strongly suggesting that NTT-$OH_{8,6}$ and NTT-no$OH_{8,6}$ have some sort of bent configurations.

Table 2. The layer thickness in the SmA phase of $OH_{m,n}$ and no$OH_{m,n}$, along with the calculated molecular length of each all-*trans*-configuration.

Compound	Exp.(SmA)/Å	Calc.(all-*trans*)/Å
NTT-$OH_{8,6}$	31.5	38
NTT-no$OH_{8,6}$	32.6	38
NTT-$OH_{6,2}$	29.1	31
NTT-no$OH_{6,2}$	30.4	31

4. Discussion

4.1. *Analysis using conventional methods* [2, 3, 4]

As we have shown above, the compounds $OH_{m,n}$ and no-$OH_{m,n}$ exhibit IR absorbance characteristics which depend significantly on the presence of OH, but depend little on chain length. On the other hand, the layer thicknesses obtained in the X-ray diffraction measurements depend on the presence or absence of the OH group, and are very different for compounds with different chain lengths. Therefore, we cannot make a straightforward interpretation about the IR absorption characteristics based on the X-ray experiments. We will therefore first analyse the polarized IR data to obtain the mean directions of the C=O stretching vibration transition moments and their order parameters. Then, we will show how the differences in the molecular conformation and hence in the direction of the transient moments affect the polar absorption patterns in the compounds $OH_{m,n}$ and no$OH_{m,n}$.

Figure 6 defines the laboratory (X, Y, Z) and molecular (x, y, z) coordinate systems. We define the angle θ as the molecular tilt angle from the layer normal (Z-axis), β as the angle between the transition moment of the C=O bond and the molecular long axis (z-axis), and Ψ as the angle between the tilt plane (Z-X) and the projection

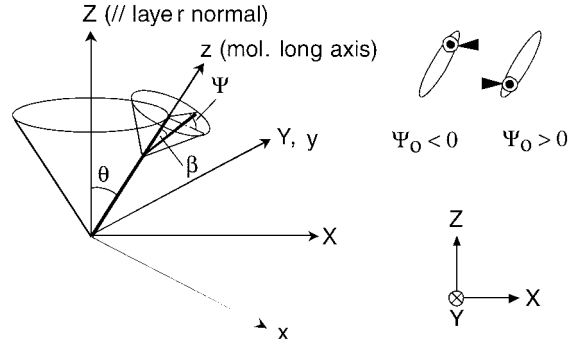

Figure 6. Coordinate systems: (X, Y, Z) defines the fixed laboratory frame, with Z taken as the layer normal and X the propagation direction of the incident light; (x, y, z) defines the molecular frame, where z is the molecular long axis. We define β as the angle between the transition moment of the C=O bond and the molecular long axis (z-axis), and Ψ as the angle between the tilt plane (Z-X) and the projection of the transition moment onto the plane perpendicular to the molecular long axis. Orientations t and b occur with equal probability because of the two fold axis of symmetry along y.

of the transition moment onto the plane perpendicular to the molecular long axis. To calculate the transition moment direction (β), we can use the normalized absorbance anisotropy D defined as,

$$D \equiv \frac{A_{\parallel} - A_{\perp}}{A_{\parallel} + 2A_{\perp}} \quad (1)$$

where $A_{\parallel}$ and $A_{\perp}$ are the absorbances for $\Omega = 0°$ and $\Omega = 90°$, respectively. In the SmA phase, where molecules rotate freely about their long axes, the absorbance (A) and order parameter (S) are related by [4]

$$A(\beta, \Omega) = -\log(10^{-A_{\parallel}} \cos^2 \Omega + 10^{-A_{\perp}} \sin^2 \Omega) \quad (2)$$

$$S = \langle P_2(\theta) \rangle = \frac{3\langle \cos^2 \theta \rangle - 1}{2} = \frac{2D}{3 - D} \quad (3)$$

where θ is an angle between the director and the molecular long axis,

$$A_{\parallel} = k(\cos^2 \beta \langle \cos^2 \theta \rangle + \sin^2 \beta \langle \sin^2 \theta \rangle / 2) \quad (4)$$

$$A_{\perp} = k(\cos^2 \beta \langle \sin^2 \theta \rangle + \sin^2 \beta \langle \cos^2 \theta \rangle / 2 + \sin^2 \beta / 2)/2 \quad (5)$$

and k is a constant of proportionality. Substituting equations (4) and (5) into (1) we can calculate D vs. β in the SmA phase. Examples with various values of $S = 0.7$, 0.4 and 0.03 are shown in figure 7. Table 3 summarizes ratios (D) and order parameters for three C=O stretching peaks. IR data show that the dichroic ratios and the carbonyl transition moment orientations do not change much between the 6, 2 and 8, 6 tail lengths. Since the X-ray data indicate that the molecules are bent, this must mean that the bend is not in the core region, but more likely where the tails join the core. $S_{\text{ph }1604}$ is computed from the observed dichroic ratio of the phenyl ring stretching (1604 cm^{-1}). We should note however that $S_{\text{ph }1604}$ for $OH_{m,n}$ is smaller than that for $noOH_{m,n}$ and that the value of about 0.4 for $OH_{m,n}$ is rather small, compared with the value of more than 0.5 for $noOH_{m,n}$. A possible explanation of this small order parameter is the overlapping of some peaks with negative D at 1604 cm^{-1} due to the existence of the hydrogen bond. Actually, two additional peaks at 1635 and 1590 cm^{-1} which are hardly seen in $noOH_{m,n}$ appear in $OH_{m,n}$. The origin of these two peaks was initially not understood. As we will show below, these are carbonyl and phenyl peaks shifted by hydrogen bonding. Moreover, if we estimate the order parameter ($S_{\text{ph }1520}$) using a peak (1520 cm^{-1}) which is related to a C–C stretching and has a large positive dichroic ratio, the difference in $S_{\text{ph }1520}$ of $OH_{m,n}$ and $noOH_{m,n}$ is actually smaller than that of $S_{\text{ph }1604}$.

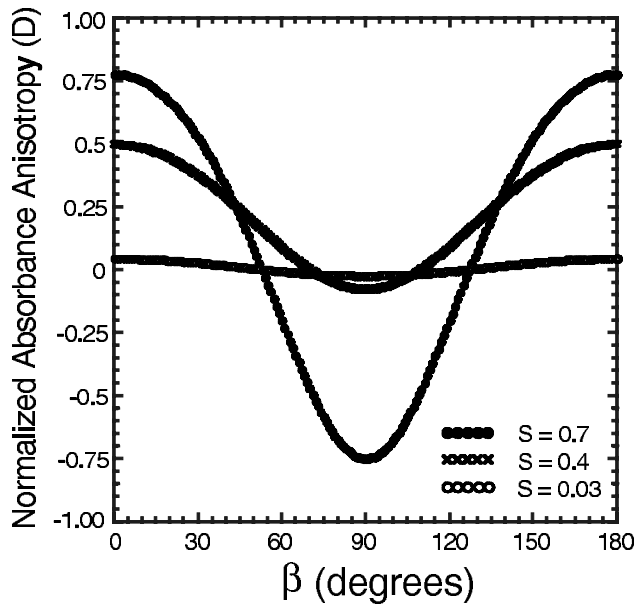

Figure 7. Calculated normalized absorbance anisotropy D as a function of the angle β between transition moment and molecular long axis in the SmA phase with $S = 0.7$, $\beta = 0°$, $S = 0.4$, $\beta = 22°$ and $S = 0.03$, $\beta = 45°$.

Let us now estimate the transition moment direction (β) of the three C=O stretching modes by comparing the experimental dichroic ratio in the SmA phase (table 3) with figure 7, where the dichroic ratios are calculated for respective values of S. The β values for the keto, ester and lactic C=O stretching directions are shown in table 4, where the results using $S_{\text{ph }1604}$, $S_{\text{ph }1520}$ (table 3) and $S = 1$ are shown. For the $OH_{m,n}$ compounds, we do not use the order parameter (S) obtained

Table 3. Normalized absorbance anisotropy D, and order parameter, S, of the three C=O groups at different T. The two order parameters, $S_{\text{ph }1604}$ and $S_{\text{ph }1520}$, specify the values determined using 1604 and 1520 cm^{-1} absorption peaks, respectively.

Compound	Temp./°C	$S_{\text{ph }1604}$	$S_{\text{ph }1520}$	D(keto)	D(ester)	D(lactic)
NTT-$OH_{8,6}$	43.0	0.42	0.55	0.37	−0.06	−0.62
NTT-$noOH_{8,6}$	69.5	0.56	0.61	−0.21	−0.1	−0.64
NTT-$OH_{6,2}$	57.0	0.31	0.50	0.28	−0.10	−0.62
NTT-$OH_{6,2}$	55.0	0.33	0.54	0.29	−0.12	−0.64
NTT-$noOH_{6,2}$	90.0	0.51	0.62	−0.23	−0.18	−0.69
NTT-$noOH_{6,2}$	60.0	0.55	0.68	−0.25	−0.21	−0.75

Table 4. β values of the three C=O groups obtained using $S_{ph\,1604}$, $S_{ph\,1520}$ and $S = 1$.

Compound	β(keto)/°	β(ester)/° using $S_{ph\,1604}$	β(lactic)	β(keto)/°	β(ester)/° using $S_{ph\,1520}$	β(lactic)	β(keto)/°	β(ester)/° using $S = 1$	β(lactic)/°
NTT-$OH_{8,6}$	28.4	58.9	Over	35.1	57.9	Over	44.0	56.5	71.0
NTT-no$OH_{8,6}$	68.1	63.2	Over	65.6	61.7	Over	61.2	59.0	72.5
NTT-$OH_{6,2}$	28.4	63.4	Over	38.8	60.0	Over	46.6	57.3	71.2
NTT-no$OH_{6,2}$	67.5	65.0	Over	64.8	62.9	Over	61.4	60.2	75.0

from the phenyl ring stretching (1604 cm^{-1}) to obtain β values because this stretching is not parallel to the molecular long axis ($\beta \neq 0$) as will be discussed in the next section, but we have to use the order parameter obtained from other phenyl ring stretching (1520 cm^{-1}). According to the results using $S_{ph\,1520}$, β of the keto C=O stretching in $OH_{m,n}$ is estimated to be small ($\beta \sim 35°$–$40°$) compared with that in no$OH_{m,n}$ ($\beta \sim 65°$), while for the ester C=O stretching these are almost the same ($\beta \sim 60°$–$63°$ for $OH_{m,n}$, and no$OH_{m,n}$).

4.2. *Effect of hydrogen bonding on the direction of the transition moment*

As mentioned above, we have observed an unusual absorbance profile for the keto C=O stretching in materials where the phenyl has an OH: maximum absorbance occurs for $\Omega = 0°$ in the SmA phase, and the presence of the OH reduces the phenyl order parameter by 10% (NTT-$OH_{8,6}$ and NTT-no$OH_{8,6}$) and 20% (NTT-$OH_{6,2}$ and NTT-no$OH_{6,2}$).

To interpret this unusual behaviour and the low dichroic ratio of the phenyl ring stretching in OH-containing compounds quantitatively, we allow the direction of the transition moment to be changed by the introduction of hydrogen bonding in our model. The calculation method is based on quantum chemical methods which have been widely applied to the electronic structure of infinitely extended solids. We use Hartree–Fock (HF) and Density Functional Theory (DFT) with Becke's three-parameter exchange functional and the gradient-corrected functional of Lee, Yang and Parr (B3-LYP DFT) [9] for geometry optimization and for the IR vibrational frequency of transition moment calculations for the keto carbonyl with and without hydroxyl on the phenyl ring. All quantum mechanical calculation employed the standard 6-31G(d) and standard 6-31G(d,f) basis sets and were performed using the GAUSSIAN94/DFT program [10]. Table 5 compares the experimental and the calculated wave numbers, which agree well.

For the case of the keto C=O without hydrogen-bonded OH, the calculated direction of the transition moment obtained from atomic vibrational displacements and charges is slightly rotated from the direction of the molecular bond axis ($\beta \sim 67°$) as shown in figure 8 (*a*).

Table 5. Experimental and calculated IR absorption peaks for keto with and without hydrogen bonding, ester and lactic carbonyl groups. The vibrational frequencies and transition moment directions were calculated using Density Functional Theory (DFT) with the Becke's three-parameter exchange functional and the gradient-corrected function (B3-LYP DFT) with the 6-31G(d) basis set.

Carbonyl group	Experimental/cm^{-1}	Calculated/cm^{-1}
Keto	1680	1690
H-bonded keto	1636	1635
Ester	1736	1739
Lactic	1770	1763

However, for the keto C=O with an intramolecular hydrogen-bonded OH, the calculated frequency of the C=O stretching is reduced to 1636 from 1680 cm^{-1} and the calculated direction of the transition moment of the keto C=O is rotated by $\sim 35°$ from the bond direction connecting C and O atoms toward the molecular long axis as shown in figure 8 (*b*). In this case, the resultant transition moment direction of the keto C=O stretching is $\beta = 25°$ from the molecular long axis instead of along the C=O bond direction ($\beta = 60°$). Any value of $\beta < 54.7°$ gives a maximum absorbance in the SmA phase, when the incident light is polarized parallel to the smectic layer normal, and $\beta = 25°$ gives an order parameter of 0.4. It is generally accepted [11] that due to hydrogen-bonding, not only are the frequencies reduced, but also the transition moment direction associated with the vibrational mode of the C=O rotates towards the direction of the hydrogen bond because the vibration is confined to an oscillation of the hydrogen atom in the bond direction and the associated transition moment direction will be almost parallel to it. The changes of polarized absorbance profiles due to hydrogen-bonding, and inter- and intra-molecular interactions in ferroelectric liquid crystal cells will be discussed experimentally and theoretically elsewhere [12].

For the case of phenyl stretching without a hydrogen-bonded OH, the calculated direction for the transition moment of the phenyl group is slightly rotated away from the molecular long axis ($\beta \sim 6°$). However, the lower phenyl dichroic ratio of the compounds with

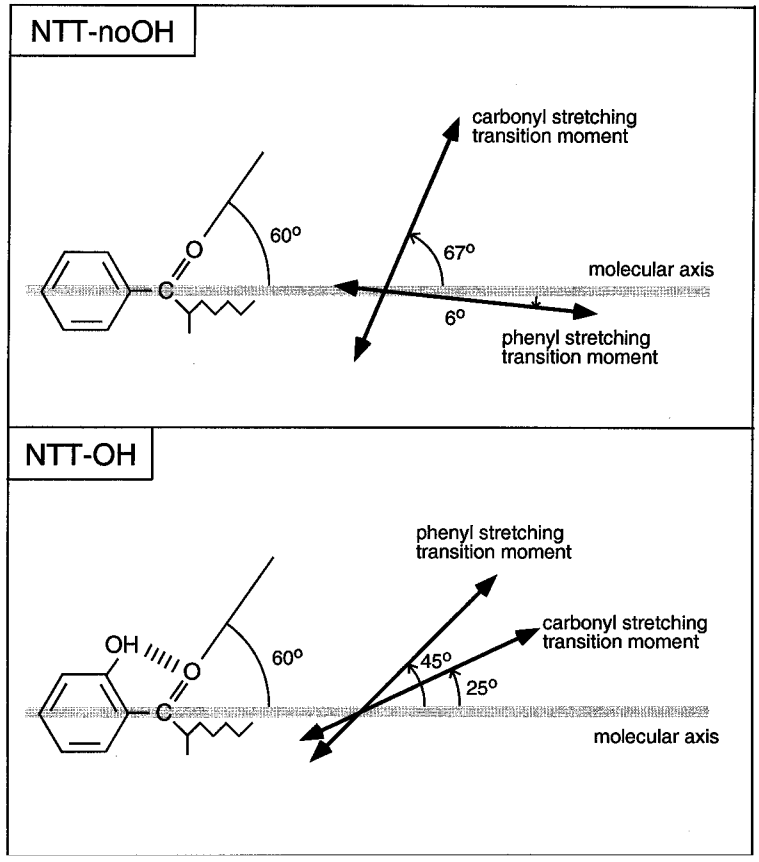

Figure 8. Calculated directions of the transition moments of phenyl and keto C=O stretching (*a*) without, (*b*) with hydrogen-bonded OH.

hydrogen-bonded OH is also caused by the fact that the phenyl absorption dipole of the phenyl containing the OH group is rotated, according to our calculations, by $\beta = 45°$ away from the molecular long axis. An assumption that the observed 1604 cm^{-1} phenyl stretching peak is a composite of the biphenyl moiety with $S = 0.7$ ($\beta = 0°$) and correspondingly high dichroism, and the phenyl ring containing OH with $S = 0.03$ ($\beta = 45°$) and low dichroism, reproduces the experimentally observed polar absorption pattern with intermediate dichroism as shown in figure 9. The unusual results described above can thus be ascribed to the change in the direction of the transition moment resulting from the C=O ... H−O hydrogen bonding. The layer thickness of the long alkyl chain compounds (NTT-$OH_{8,6}$ and NTT-no$OH_{8,6}$) measured by X-ray diffraction are much smaller than the estimated thickness assuming all-*trans*-molecules, suggesting that the molecules are bent, while the layer spacings of NTT-$OH_{6,2}$ and NTT-no$OH_{6,2}$ agree with those of all-*trans*-molecules.

Thus the IR dichroism results show that the 8, 6 materials are bent, and the bend is not in the core, since, apart from hydrogen-bonding effects, the dichroic ratios are nearly the same for the 6, 2 and 8, 6 compounds. Gaussian94 calculations of low energy conformations

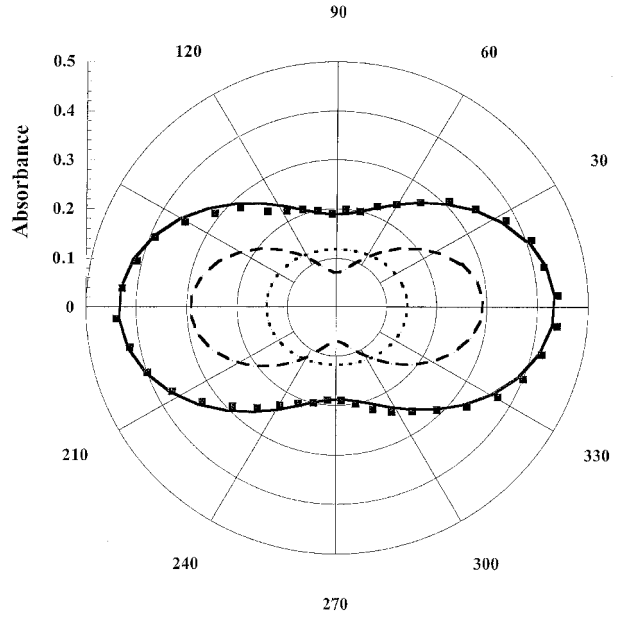

Figure 9. Experimentally observed polar absorption pattern (■) with intermediate dichroism for the 1604 cm^{-1} phenyl stretching peak fitted (solid) with a composite of the biphenyl (long dashes) with $S = 0.7$ ($\beta = 0°$) and a correspondingly high dichroism, and the phenyl containing OH (short dashes) with $S = 0.03$ ($\beta = 45°$) and a low dichroism.

indicate that the bend is in the tails, near where they join the core. Specifically, it is found [13] that the first two bonds in the tail (O=C−C*−C and O=C−C*−O bonds tend to be *gauche* in the lowest energy conformations, leading to an almost 90° bend there in the molecules) provide bent conformations in much the same fashion as is found for the O=C−O−C*−C methyl oxy tail of MHPOBC [14]. This kind of tail bend can clearly account for the reduced length of the 8, 6 homologues.

4.3. *Orientational bias in SmC**

In the SmC* phase, as a result of the lack of mirror symmetry, the most probable orientation of the C=O group is $\Psi = \Psi_0 \neq 0°$. It should be noted that the overall C=O group orientational distribution is symmetric under the operation $\Psi \rightarrow -\Psi$ (figure 6), because of the head-and-tail equivalence of the molecular orientation. Therefore, the azimuthal distribution function of the carbonyl group about the molecular axis in the biased rotational motion may be described [2] by

$$f(\Psi) = f_t(\Psi) + f_b(\Psi) = f_t(\Psi) + f_t(-\Psi)$$
$$= \left(\frac{1}{2\pi}\right)\{2 + a[\sin(\Psi - \Psi_0) + \sin(\Psi + \Psi_0)]\}. \quad (6)$$

Here a is the degree of bias and the subscripts t and b stand for the two molecular orientations related by a π rotation about y, respectively, as illustrated in figure 6; we have kept only the lowest order sinusoid in the Fourier expansion in $\Psi - \Psi_0$. In general the absorbance vs. polarizer rotation angle, $A(\Omega')$, is given by

$$A(\beta, \Omega') = -\log(10^{-A_\parallel}\cos^2\Omega' + 10^{-A_\perp}\sin^2\Omega') \quad (7)$$

where $\Omega' = \Omega - \delta$, $A_\parallel = k\langle P_\parallel^2\rangle$, $A_\perp = k\langle P_\perp^2\rangle$ and δ is the tilt angle determined as half the difference between Ω_{max} of the phenyl stretching in the SmC* phase under positive and negative voltages. The relations between the absorbances $A_\parallel$ and $A_\perp$ in the molecular frame and the absorbances A_Z, A_Y and A_{YZ} in the fixed laboratory frame are as follows:

$$A_Z = A_\parallel \cos^2\delta + A_\perp \sin^2\delta \quad (8)$$

$$A_Y = A_\parallel \sin^2\delta + A_\perp \cos^2\delta \quad (9)$$

$$A_{YZ} = \sin\delta\cos\delta(A_\parallel - A_\perp) \quad (10)$$

where A_Z, A_Y and A_{YZ} are related to the rotational reorientation distribution function obtained before [4]

$$A_Z = k(\cos^2\beta\langle\cos^2\theta\rangle - 2\sin\beta\cos\beta\langle\sin\theta\cos\theta\rangle\langle\sin\psi\rangle + \sin^2\beta\langle\sin^2\theta\rangle\langle\sin^2\psi\rangle)$$

$$A_Y = k(\cos^2\beta\langle\sin^2\theta\rangle + 2\sin\beta\cos\beta\langle\sin\theta\cos\theta\rangle\langle\sin\psi\rangle + \sin^2\beta\langle\cos^2\theta\rangle\langle\sin^2\psi\rangle)$$

$$A_{YZ} = k[\langle\sin\theta\cos\theta\rangle(\cos^2\beta - \sin^2\beta\langle\sin^2\psi\rangle) + \sin\beta\cos\beta(\langle\cos^2\theta\rangle - \langle\sin^2\theta\rangle)\langle\sin\psi\rangle]. \quad (11)$$

The difference between Ω'_{max} of the C=O stretching in the SmA and SmC* phases, $\Delta\Omega'_{max}$, is about 0°, −26° and −4° for the keto, ester and lactic acid C=O groups, respectively. The tilt angle δ from the layer normal direction is given by

$$\delta = \frac{1}{2}\tan^{-1}\left(\frac{2A_{YZ}}{A_Z - A_Y}\right) \quad (12)$$

where A_Y, A_Z, A_{YZ} are functions of $\langle\sin\psi\rangle$ given by equation (11).

Figures 10 and 11 show δ for the ester C=O group ($\beta = 57.9°$) and lactic C=O group ($\beta = 79.9°$) as a function of the orientational bias factor $\langle\sin\psi\rangle = a\sin\Psi_0$. Here we assumed that β in SmC* is the same as that in SmA. Comparing these calculated curves with the experimental tilt angles, we obtain $\langle\sin\psi\rangle = 0.34$ and 0.11 for the ester and lactic acid C=O groups, respectively. The ester carbonyl value is unexpectedly large, implying an important contribution to the high observed $\mathbf{P}_s$ of NTT-OH$_{8,6}$.

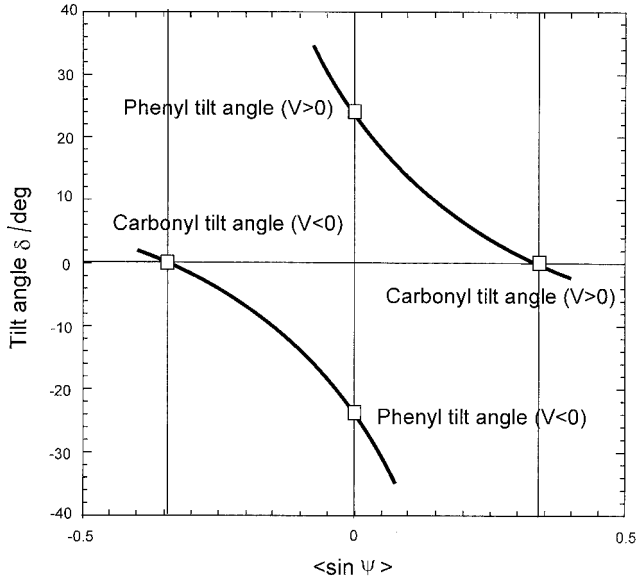

Figure 10. Calculated tilt angle δ of the ester C=O ($\beta = 57.9°$) absorption profile from the layer direction as a function of the bias factor $\langle\sin\psi\rangle$ in NTT-OH$_{8,6}$. The absence of reorientation of the profile with field reversal ($\delta \sim 0$) implies a strong orientational bias ($\langle\sin\psi\rangle = 0.34$).

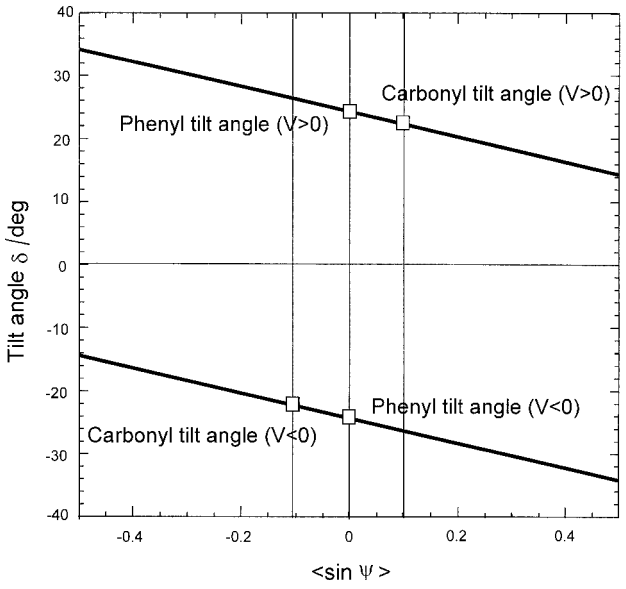

Figure 11. Calculated tilt angle δ of the lactic C=O ($\beta = 79.9°$) absorption profile from the layer direction as a function of the bias factor $\langle \sin\psi \rangle$ in NTT-$OH_{8,6}$. Again this carbonyl is orientationally biased ($\langle \sin\psi \rangle = 0.11$).

5. Conclusion

We have studied the molecular conformations of ferroelectric liquid crystals, having three C=O groups and large spontaneous polarizations, using polarized FTIR and X-ray measurements. We find that the difference in the keto C=O absorption, with and without intramolecular hydrogen bonding from OH groups on phenyl rings in the molecular core, can be attributed to hydrogen bonding. The shapes of the polarized absorbance patterns for C=O stretching in the SmC* phase suggest a significant degree of biased orientation of the ester C=O groups about the molecular long axes.

This work was supported by NSF MRSEC Grant No. DMR 98-09555, ARO Grant No. DAAGA55-98-1-0046, and AFOSR MURI F49620-97-1-0014.

References

[1] Kobayashi, S., Ishibashi, S., and Tsuru, S., 1990, *Mol. Cryst. liq. Cryst. Lett.*, **7,** 105.
[2] Kim, K. H., Ishikawa, K., Takezoe, H., and Fukuda, A., 1995, *Phys. Rev. E*, **51,** 2166.
[3] Miyachi, K., Matsushima, J., Takanishi, Y., Ishikawa, K., Takezoe, H., and Fukuda, A., 1995, *Phys. Rev. E*, **52,** R2153.
[4] Jang, W. G., Park, C. S., Maclennan, J. E., Kim, K. H., and Clark, N. A., 1996, *Ferroelectrics*, **180,** 213.
[5] Jin, B., Ling, Z., Takanishi, Y., Ishikawa, K., Takezoe, H., Fukuda, A., Kakimoto, M., and Kitazume, T., 1996, *Phys. Rev. E*, **53,** R4295.
[6] Shilov, V., Skupin, H., Kremer, F., Gebhard, E., and Zentel, R., 1997, *Liq. Cryst.*, **22,** 203.
[7] Kocot, A., Vij, J. K., and Perova, T. S., 2000, *Adv. chem. Phys.*, **113,** 203.
[8] Hide, F., Clark, N. A., Nito, K., Yasuda, A., and Walba, D. M., 1995, *Phys. Rev. Lett.*, **75,** 2344.
[9] Lee, C., Yang, W., and Parr, R. G., 1988, *Phys. Rev. B*, **785,** 37.
[10] Frisch, M. J. *et al.*, 1994, Gaussin 94, Gaussin, Inc., Pittsburgh PA, USA.
[11] Colthup, N. B., Daly, L. H., and Wilberley, S. E., 1964, *Introduction to Infrared and Raman Spectroscopy* (Academic Press).
[12] Jang, W. G., Park, C. S., Kim, K. H., Glaser, M. A., and Clark, N. A., 2000, *Phys. Rev. E*, **62,** 5027.
[13] Nendel, M., Glaser, M. A., and Walba, D. M., unpublished results.
[14] Jin, B., Ling, Z., Takanishi, Y., Ishikawa, K., Takezoe, H., Fukuda, A., Kakimoto, M., and Kitazume, T., 1996, *Phys. Rev. E*, **53,** R4295.